Structural Engineering and Mechanics, *Vol. 47, No. 4 (2013) 531-544*
DOI: http://dx.doi.org/10.12989/sem.2013.47.4.531

Effects of traffic characteristics on pavement responses at the road intersection

Qun Yang* and Jingwang Dai

Key Laboratory of Road and Traffic Engineering of the Ministry of Education, Tongji University, Shanghai 201804, China

(Received February 23, 2012, Revised August 10, 2013, Accepted August 16, 2013)

Abstract. Compared with pavement structures of ordinary road sections, pavement structures in the intersection are exposed to more complex traffic characteristics which may exacerbates pavement distresses such as fatigue-cracking, shoving, shear deformation and rutting. Based on a field survey about traffic characteristics in the intersection conducted in Shanghai China, a three dimensional dynamic finite-element model was developed for evaluating the mechanistic responses in the pavement structures under different traffic characteristics, namely uniform speed, acceleration and deceleration. The results from this study indicated that : (1) traffic characteristics have significant effects on the distributions of the maximum principal strain (MPS) and the maximum shear stress (MSS) at the pavement surface; (2) vehicle acceleration or deceleration substantially impact the MPS and MSS at pavement surface and could increase the magnitude of them by 20 percent to 260 percent; (3) in the vertical direction, with the increase of vehicle deceleration rate, the location of the MPS peak value and the MSS peak value changes from the sub-surface layer to the pavement surface.

Keywords: intersection area; traffic characteristic; dynamic finite element; maximum principal strain; maximum shear stress

1. Introduction

Road intersection is the hub of urban transportation where vehicles and pedestrians merge into each other, making the traffic characteristics very complex in this area. With vehicles braking and starting frequently, more serious distresses appear in pavement structures of the intersection compared with ordinary road sections. In recent years, the increase of traffic volume, axle load and tyre pressure has been causing more serious pavement distresses (shoving, rutting, fatigue cracks, etc.) in some metropolises of China. According to a field investigation conducted by Ma (2009), surface layer in the intersection should be rebuilt every two years. To improve the road conditions in the intersection, the mechanistic responses in pavement structures considering different traffic characteristics need to be evaluated.

Methods to evaluate pavement mechanistic responses can be grouped into two categories namely elastic dynamic method and numerical method. In the 1950s, some researchers in the elastic dynamics field evaluated road dynamics considering elastic homogeneous space,

*Corresponding author, Associate Professor, E-mail: qunyang.w@tongji.edu.cn

http://www.techno-press.org/?journal=sem&subpage=8 ISSN: 1225-4568 (Print), 1598-6217 (Online)

semi-space or single plate (Sneddon 1952, Fuhon *et al*. 1956, Mandel *et al*. 1961). With the development of numerical method and the improvement of computer capacity, researchers converted to explain pavement distresses by developing analytical models. Different assumptions could be applied in the model such as that asphalt materials might be elastic or viscoelastic and load could be static or dynamic. Siddharthan *et al*. (1998) developed an analytical model to evaluate the responses of asphalt pavement under moving load assuming that the pavement structure consisted of a serious of elastic layers of the same nature. Numerical models, developed with the help of finite element softwares, are able to analyze the mechanistic responses in pavement structure more efficiently and make it possible to take more flexible conditions into account. Wang and Al-Qadi (2009) evaluated the influence of 3-D contact stress and dynamic loading on the mechanistic responses in pavement structures. They took the viscoelastic feature of asphalt concrete into account. Hernandez (2010) compared the results of finite element analyses with those calculated by the MEPDG (Mechanistic-Empirical Pavement Design Guide) method and the experimental data. Hu (2011) achieved to model the pavement mechanistic responses in the AC layers by simulating different layer interfacial bonding conditions (namely fully bonded and debonded). The applied load was based on the actual measured tyre-pavement contact pressure.

Existing analytical models based on finite element method have achieved to evaluate pavement mechanistic responses accurately. Nevertheless, different loading scenarios are presumed: one is the change in the vehicle speed leading to different loading time and the other is the change of horizontal pressure due to vehicle acceleration. Actually when non-uniform speed is considered, both of the above scenarios should be considered. However few literatures considered loading time as well as horizontal pressure.

The objective of the present study is to evaluate the pavement mechanistic responses and to reveal the intrinsic mechanism of pavement distresses at the road intersection. Based on the field survey about driving characteristic in Shanghai China, a dynamic finite element model is developed. Both loading time and horizontal contact pressure are considered. By comparing the MPS and MSS considering different traffic characteristics, this paper achieves to explain about pavement distresses at the road intersection.

2. Three-dimensional dynamic finite element model

This paper focuses on pavement structures with semi-rigid base layer, which is recommended by the specifications for asphalt pavement design of China. Vehicle load is assumed as moving surface load. A three-dimensional finite element model is developed to analyze the mechanistic responses in pavement structures considering different loading scenarios.

2.1 Parameters of the model

Parameters of the finite element model conclude the modulus of each material, driving characteristics at the intersection, tyre-pavement contact pressures etc. The parameters were determined based on field surveys and related literatures.

2.1.1 Traffic characteristics in the intersection

Parameters about traffic characteristics mainly conclude the typical speed and acceleration of

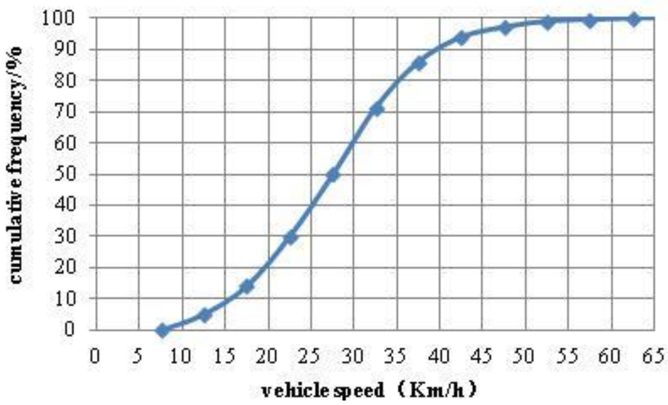

Fig. 1 Cumulative frequency curve of vehicle speed for the entrance lane

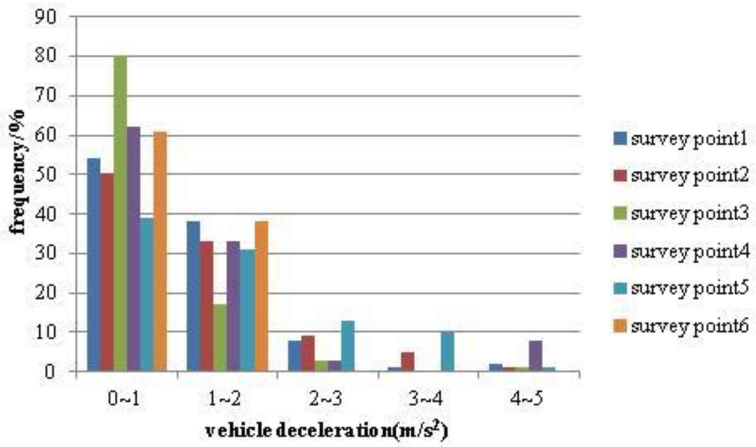

Fig. 2 Deceleration distribution for the entrance lane

vehicles at the intersection. A field survey about traffic volume and traffic characteristics was conducted in Shanghai, China. Six typical intercourses were chosen. Generally, research works about pavement mechanistic analysis only focus on trucks with greater than 2.5t load capacity and buses with more than 40 seats (Al-Qadi 2009, Hernandez 2010). Therefore, the field survey about traffic characteristic in this paper only refers to heavy trucks. The cumulative frequency curve of vehicle speed in the entrance lane is presented in Fig. 1. The acceleration distribution of vehicles in the entrance lane is shown in Fig. 2.

From Fig. 1, it can be seen that the 50 percent quantile of the cumulative frequency curve is 28 km/h. This value is used as the typical speed of the dynamic model in the following finite element analyses. According to Fig. 2 the vehicle decelerations in the entrance lane concentrates in the region of 0~2 m/s^2. The measured maximum vehicle deceleration is $5m/s^2$. Much research work has revealed that greater vehicle deceleration has significant influence on the fatigue life of pavement structures (Hu 2011, Dong *et al*. 2011). To evaluate the influence of vehicle deceleration rate on pavement responses, $2m/s^2$, $4m/s^2$, and $6m/s^2$ decelerations are considered in this study. According to 'Guide for Highway Design' of China, the expected acceleration for trucks is 2~2.5

Table1 Layer material properties for pavement structures

Structural layer	Thickness (cm)	Modulus (MPa)	Poisson's ratio
Wearing layer	5	3900	0.35
Subsurface layer	6	4900	0.35
Binder layer	8	5600	0.35
Semi-rigid base	40	3800	0.2
Sub base	20	3000	0.2
The soil	--	130	0.4

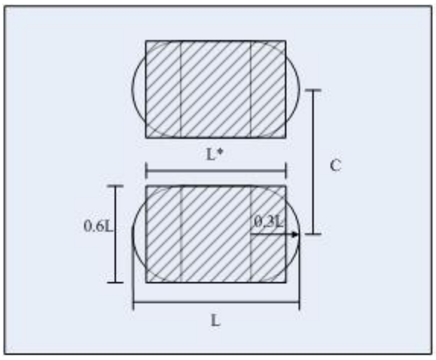

Fig. 3 Tyre-pavement interaction area model

m/s^2. So 2m/s^2 vehicle acceleration is considered in this study. Initial velocities of finite element models considering vehicle acceleration and deceleration are assumed at 28km/h, in accordance with that considering constant vehicle speed.

2.1.2 Material properties for pavement structures

In order to simulate the pavement structures under moving load, dynamic modulus of each layer is determined. According to the results of AI method (Zhang 2006), the average dynamic modulus of asphalt mixtures is 4000MPa. The testing results achieved by Wang (2002) indicate that, when the loading frequency is 5Hz and the temperature is 20℃, the dynamic modulus is 3100MPa for dense gradation asphalt concrete gravel and 3500MPa for hot-rolled asphalt concrete. Yang (2007) studied the dynamic modulus of several kinds of asphalt mixtures. The values range of dynamic modulus (10Hz, 20℃) is 5500MPa~8500MPa for AC20, 5500MPa~7500MPa for AC16, 5000MPa~6000MPa for AC16F.

In this study the dynamic modulus of each structural layer (listed in Table 1) are determined according to the above research achievements. The thickness of each structural layer is determined by the typical pavement structure compositions in Shanghai, China.

2.1.3 Tyre-pavement interaction model

Tire-pavement contact stress distributions are usually complex and different from the theory about multilayer elastic system that assumes circular contact area (Specifications for Design of Highway Asphalt Pavement). In fact the contact area is more approximate to rectangle, especially when higher axle loads are considered. The contact area model adopted in this study is shown in Fig. 3.

The length of the tyre-pavement interaction area model is L, the width is 0.6L, and the contact area is A_0. The tyre footprint is the combination of a rectangular area (0.4L×0.6L) and two semicircular area (the radius is 0.3L). The equation to calculate the area is given by

$$A_0 = \pi \times (0.3L)^2 + 0.4L \times 0.6L \tag{1}$$

$$L = \sqrt{\frac{A_0}{0.5227}} \tag{2}$$

The length of the equivalent rectangular area can be expressed as

$$L^* = \frac{A_0}{0.6L} \tag{3}$$

The centric distance of two tyre footprints (C) is: C=1.5D_0. In this equation, $D_0 = \sqrt{4A_0 / \pi}$, which is the diameter of the equivalent round load. The equation to calculate 'C' becomes: $C = \sqrt{9A_0 / \pi}$.

The centric distance of two tyre footprints is assumed at 32cm in this study, and the contact stress is assumed at 0.7Mpa, the standard tyre inflation pressure of heavy trucks. The length and width of the tyre footprint are 22cm and 16.2cm. Ma (2005) made a research about the influence of tyre-pavement interaction area on the mechanistic responses. It was proved that the shape of contact area and the contact stress have little influence on the mechanistic responses in pavement structures. So the same tyre-pavement interaction model is used in the following finite element models.

2.2 Dynamic finite element model considering uniform vehicle speed

In ordinary road sections, it is assumed that vehicles travel at constant speed. Along with the vertical vehicle load, the surface layer of asphalt pavement is exposed to the rolling friction of the tyre also. However the rolling friction when vehicles travel at constant speed is much lower compared with the vertical load, which is below 5% of the vertical load. Therefore the rolling friction is ignored in this part, and the applied load is valued at the standard axle load (100MPa). The loading speed is assumed at 28km/h.

In order to simulate the moving load, a quasi-static analysis was carried out (Hernandez 2010). The position of the load is continuously changed a distance equal to the length of the contact area. The duration of each load step is the length of the contact area divided by the moving speed. Therefore the moving procedure of the applied load is simplified as following: the wheel path of dual tyre is divided into 30 parts by the length of the contact area (22cm); the load is applied at the first section and the model is calculated; then the load at the first section is removed and the same load is applied at the second section; repeat the above procedure until the load is applied at the last section. The division of the wheel path is shown in Fig. 4.

2.3 Dynamic finite element model considering vehicle acceleration and deceleration

In the intersection area, the distribution of tyre-pavement contact pressures is complex for

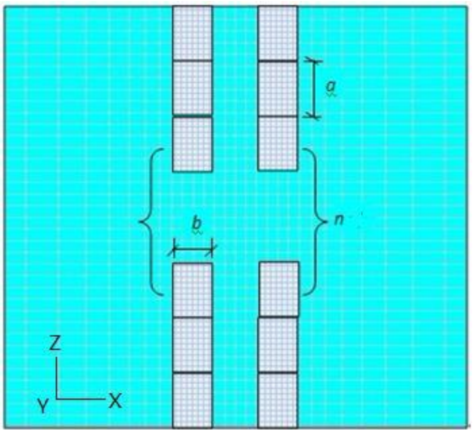

Fig. 4 Moving procedure of the applied load

vehicles travel at variational speed. In order to simplify the numerical model, the vehicle load is assumed to be the combination of vertical uniform distributed load and horizontal rectangular load. The vertical part component is the standard axle load, and the horizontal component is calculated by the following formula.

$$F = \delta P \tag{4}$$

Where: F=the horizontal load; δ=scale factor, it is the ratio of acceleration (a) and acceleration of gravity (g); P=the vertical load.

The moving procedure of the load is same to that considering constant vehicle speed. The duration for each load step is calculated by the initial velocity and the vehicle acceleration. Assuming that the vehicles brake from the initial velocity (v_0) to v_n (the acceleration is a), then the procedure is expressed by

$$V_n = V_0 - at_n \Rightarrow t_n = \frac{V_0 - V_n}{a} \tag{5}$$

$$-2an\Delta S = V_n^2 - V_0^2 \tag{6}$$

$$V_n = \sqrt{V_0 - 2an\Delta S} \tag{7}$$

$$V_{n-1} = \sqrt{V_0 - 2a(n-1)S_{n-1}} \tag{8}$$

$$\Delta t = t_n - t_{n-1} = \frac{V_n - V_{n-1}}{a} = (\sqrt{V_0 - 2an\Delta S} - \sqrt{V_0 - 2a(n-1)S_{n-1}}) / a \tag{9}$$

Where: ΔS=the moving distance of the load step; n=the number of load steps.

The duration of each load step is calculated by Eq. (9) using the value of vehicle acceleration. The value of vehicle acceleration is negative when braking, so the duration of each load step increases one by one, thus modeling the process of braking. It is the same to the procedure of accelerating speed, the duration of each load step decreases one by one, and the model is used to modeling the acceleration process.

3. Analytical results of the three-dimensional finite element model

Based on the three-dimensional dynamic finite element model considering different traffic characteristics, the following mechanistic responses are computed and are presented in this paper:

(1) The distribution of the MPS at the pavement surface.
(2) The variation of the MPS peak value with depth.
(3) The distribution of the MSS at the pavement surface.
(4) The variation of the MSS peak value with depth.

3.1 Maximum principal strains

The influence of the dynamic traffic characteristics on the MPS distribution is presented in this section. Both vehicle acceleration and deceleration are considered. Based on the field survey about traffic volume and driving characteristic at the intersection, $2m/s^2$ acceleration and $2m/s^2$, $4m/s^2$ and $6m/s^2$ deceleration are assumed in this study. Different horizontal loads were considered according to the magnitude of acceleration or deceleration.

3.1.1 The distribution of the MPS at the pavement surface

Fig. 5 shows the contours for the MPS distribution at the pavement surface. The peak values of the MPS are marked by ‘MX’ in Fig.5, and these values are listed in Table 2. It is observed that the traffic characteristics dramatically influence the MPS distribution at the pavement surface.

From Fig. 5, it is noticed that the MPS peak value occurs between the two rectangular loading areas when uniform speed is considered. By comparing the contours considering $2m/s^2$ acceleration with that considering $2m/s^2$ deceleration, it can be noted that acceleration and deceleration have generally the same influence on the distribution of the MPS at the pavement surface; the only difference is the direction of the distribution. The MPS peak value occurs in front of or behind the tyre footprint when $2m/s^2$ acceleration or deceleration is considered. While this value both occur at the fore-end of the tyre footprint when $4m/s^2$ deceleration and $6m/s^2$ deceleration is considered. In other words, when the vehicle deceleration increases from $4\ m/s^2$ to $6m/s^2$, no significant change about the location of the peak value is found.

Table 2 presents the MPS peak values at the pavement surface considering different traffic characteristics. It is noted that acceleration and deceleration have the similar influence on the magnitude of the MPS peak value. Hu (2011) showed that, when compared with vehicle acceleration, vehicle deceleration causes more dramatic changes in the vertical shear strain at the pavement surface. However, the analytical results of this study show that this component of strains has little influence on the MPS peak value. This may be explained by the different pressure distributions.

From Table 2, it is also observed that the magnitude of deceleration has substantially influence on the MPS peak value. When $2m/s^2$ deceleration is considered, the result is 1.2 times of that considering uniform vehicle speed. When the deceleration rate increases, i.e., doubled to $4m/s^2$, the induced peak value increases by 1.8 times in magnitude. Compared to $2m/s^2$ deceleration, there is an increase of 3.0 times in magnitude when the deceleration rate increases to $6m/s^2$. It shows that

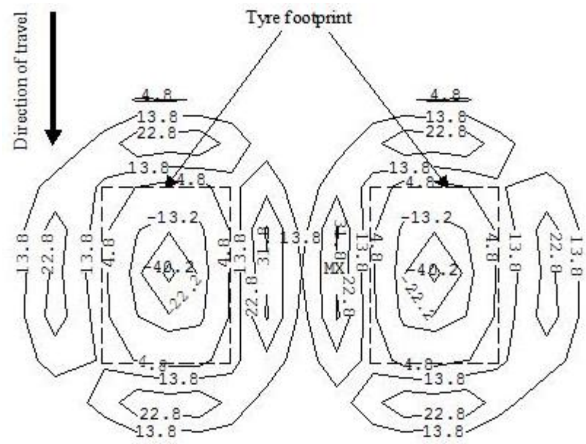

(a) Uniform speed

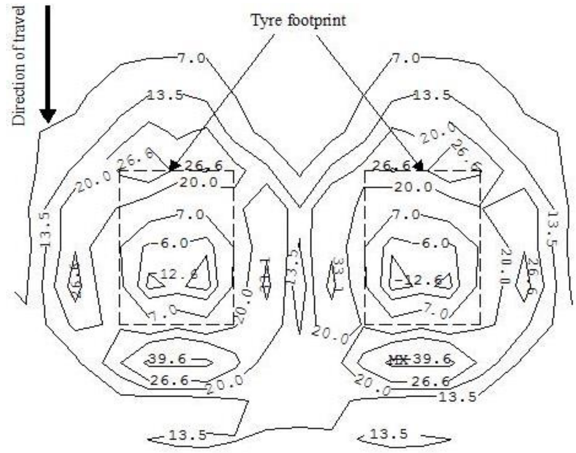

(b) $2m/s^2$ acceleration

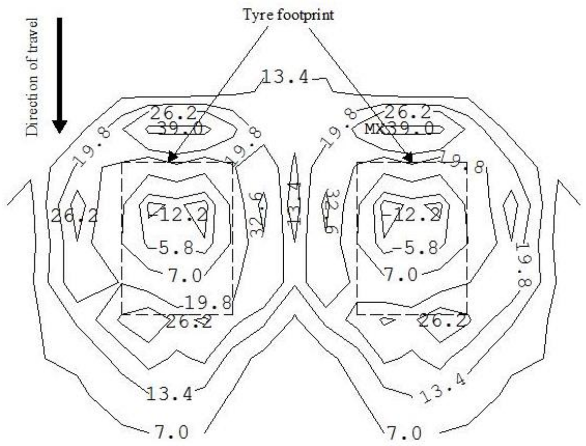

(c) $2m/s^2$ deceleration

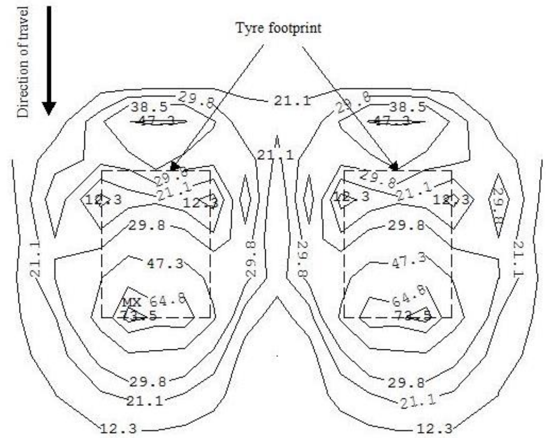

(d) $4m/s^2$ deceleration

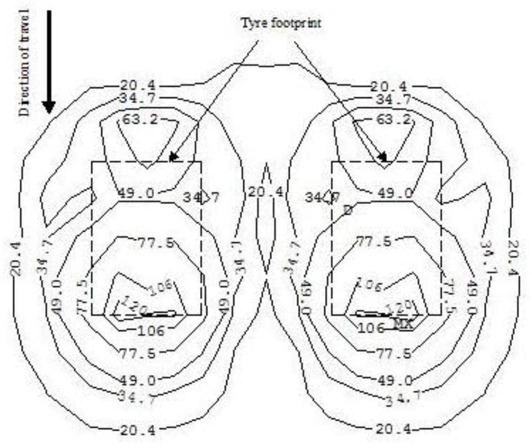

(e) $6m/s^2$ deceleration

Fig. 5 Contours of the MPS distribution

Table 2 Peak values of the MPS at the pavement surface

Traffic characteristics	MPS peak value(με)
Uniform speed	36.3
2m/s2 acceleration	42.9
2m/s2 deceleration	42.2
4m/s2 deceleration	77.9
6m/s2 deceleration	128

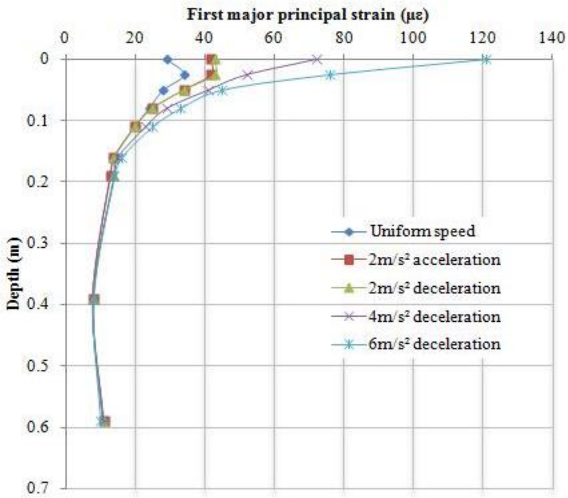

Fig. 6 Distribution of the MPS with depth

large deceleration, i.e., 6m/s^2, causes much significant MPS, which may exacerbate pavement distresses.

3.1.2 The variation of the MPS peak values with depth

The MPS peak values in each pavement layers were calculated in ANSYS, and the variation of these values with depth for different traffic characteristics is shown in Fig. 6. The maximum depth presented is 0.59m (the interface of the semi-rigid base and the sub base) because after this point, all curves approach asymptotically to zero.

It is noted that the difference between the results considering different traffic characteristics decreases as the depth increases. It is also observed that the difference below the depth of 0.2 m. for different traffic characteristics is negligible. In other words, vehicle acceleration or deceleration brings greater principal strains in the surface layer. Combined with the analysis about the MPS peak values at the pavement surface, it can be noticed that vehicle deceleration causes dramatic changes in the magnitude of the MPS in the surface layer. The above influence of acceleration and deceleration agrees with the conclusions drawn by Hu (2011).

By comparing the analytical results considering different traffic characteristics in Fig. 6, it is noted that acceleration or deceleration changes the variation tread of the MPS with depth. For uniform speed and lower deceleration in magnitude, the peak value in depth is at the interface of the wearing layer and the sub-surface layer. However, when the deceleration increases to 4m/s^2 and 6m/s^2, the peak value both occur at the pavement surface.

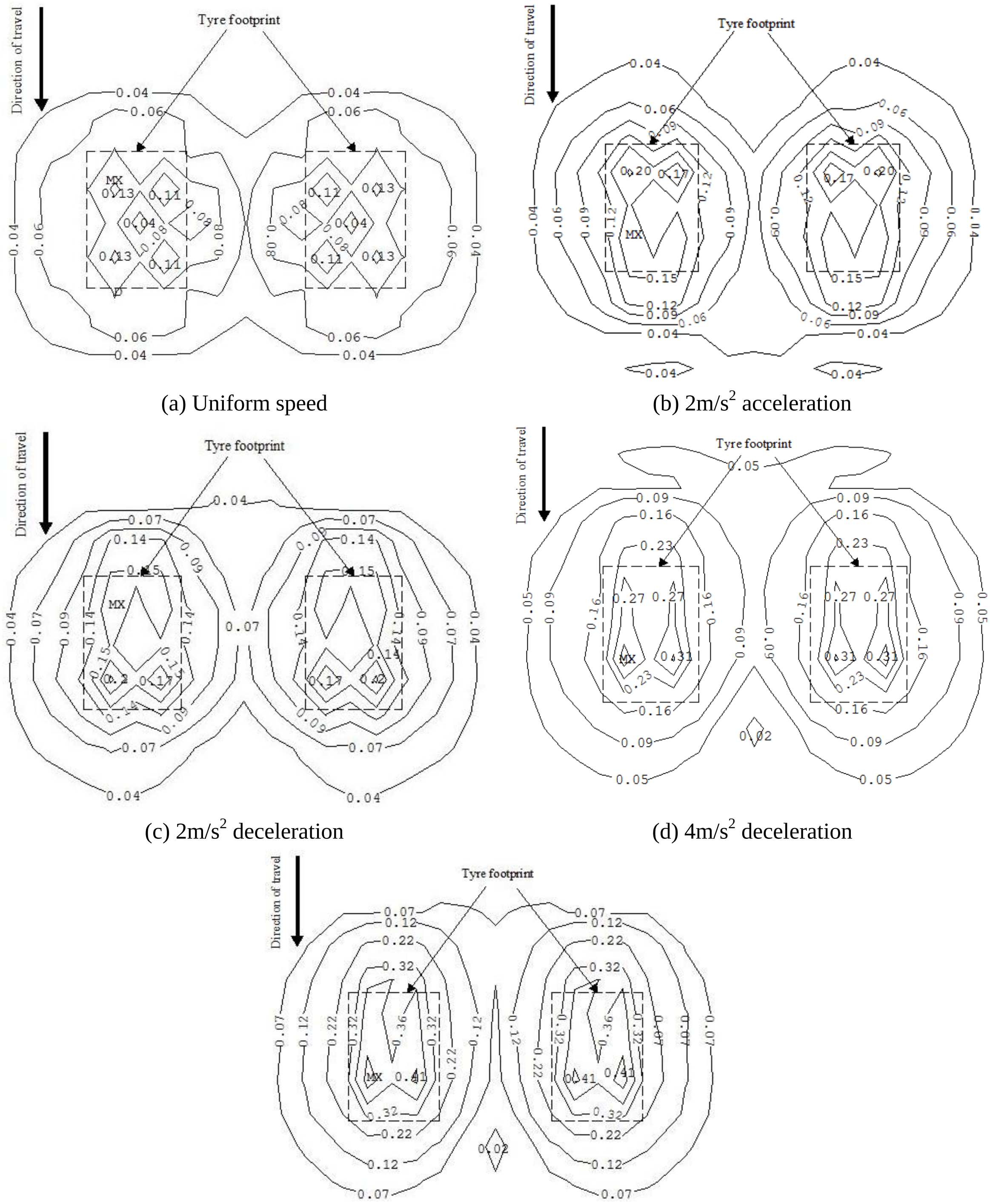

(a) Uniform speed

(b) $2m/s^2$ acceleration

(c) $2m/s^2$ deceleration

(d) $4m/s^2$ deceleration

(e) $6m/s^2$ deceleration

Fig. 7 Contours of the MSS distribution

Table 3 Peak values of the MSS at the pavement surface

Traffic characteristics	MSS peak value(Mpa)
Uniform speed	0.13
2m/s2 acceleration	0.22
2m/s2 deceleration	0.22
4m/s2 deceleration	0.31
6m/s2 deceleration	0.44

Based on the analytical results about the MPS in pavement structures, it can be inferred that: At the intersection, the complex traffic characteristics cause dramatic changes in the MPS at the pavement surface, and will theoretically have significant bearing on the pavement performance or surface distresses. It can easily lead to fatigue cracking at the pavement surface.

3.2 Maximum shear stresses

The influence of the traffic characteristics on the MSS distribution is presented in this section. Both acceleration (2m/s^2) and deceleration (2m/s^2, 4m/s^2 and 6m/s^2) are considered.

3.2.1 The distribution of the MSS at the pavement surface

Fig. 7 shows the contours for the MSS distribution at the pavement surface. The peak values of the MSS are marked by ‘MX’; these values are listed in Table 3. It is observed that acceleration or deceleration influence the MSS distribution at the pavement surface.

Different from the distribution of MPS, the MSS peak values all occur under the tyre footprint. The locations of the peak values are near to the outside of the tyre footprint in the transverse direction. However in the longitudinal direction, the locations are affected by the different traffic characteristics. When considering uniform speed or 2m/s^2 deceleration, the location of the MSS peak value is near to the rear-end of the tyre footprint. When the deceleration increases to 4m/s^2 and 6m/s^2, the locations change to the forepart of the tyre footprint. By comparing the contours considering 2m/s^2 acceleration and 2m/s^2 deceleration, it can also be noted that acceleration and deceleration have about the same influence on the distribution of the MSS at the pavement surface; the only difference is the direction of the distribution.

Table 3 presents the MSS peak values at the pavement surface. It is noted that acceleration and deceleration have the same influence on the MPS peak value. The magnitude of deceleration has substantially influence on the MSS peak value. When 2m/s^2 deceleration is considered, the result is 1.7 times of that considering uniform speed. However, when the deceleration rate increases, i.e. doubled to 4m/s^2, the induced peak value increases by 1.4 times in magnitude. Compared to 2m/s^2 deceleration, there is an increase of 2.0 times in magnitude when the deceleration rate increases to 6m/s^2.

3.2.2 The variation of the MSS peak values with depth

The MSS peak values in each pavement layers are calculated in ANSYS, and the variations of the MSS with depth considering different traffic characteristics are shown in Fig.8. The maximum depth presented is 0.79m because after this point, all curves approach asymptotically to zero. And this point is the interface of the sub base and the soil.

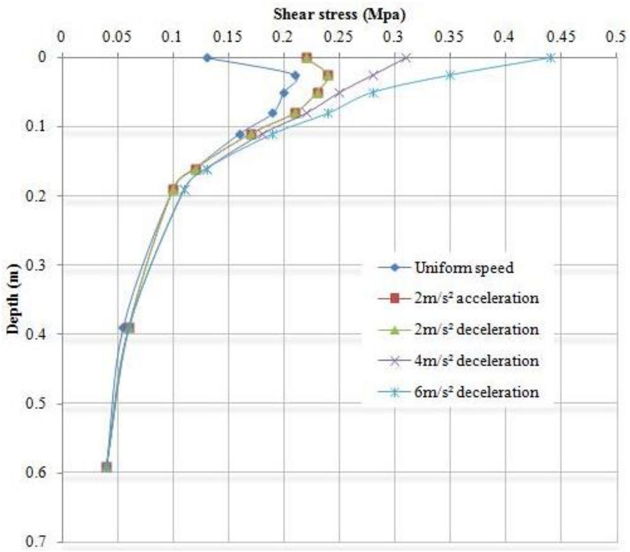

Fig. 8 Distribution of the MSS with depth

From Fig. 8, it is noted that the difference between the results considering different traffic characteristics decreases as the depth increases. The peak value when considering uniform speed appears in the sub-surface layer. However, the peak values when considering 2m/s^2 acceleration and 2m/s^2 deceleration both appear at the interface of the wearing layer and the sub-surface layer. With the increases of deceleration rate, the location of the peak values changes up to the pavement surface. And the variation rate of the MSS with depth increases when the vehicle deceleration changes from 4m/s^2 to 6m/s^2.

Based on the above analyses about MSS in pavement structures, it can be inferred that: Vehicle deceleration causes dramatic changes in the MSS in the surface layer of asphalt pavements, and the stresses are significantly influenced by the magnitude of deceleration. Therefore, vehicle deceleration (even at the intersection) is detrimental to pavement structures. It can easily lead to shear deformation with other secondary distresses such as rutting and cracking in the wearing layer or sub-surface layer.

4. Conclusions

A dynamic finite element model considering the typical traffic characteristics at the road intersection is developed in ANSYS. By comparing the mechanistic responses under different traffic characteristics and analyzing the mechanisms of pavement distresses, conclusions can be drawn as below:

(1) At the intersection, vehicle acceleration or deceleration causes dramatic changes in the distributions of the MPS and the MSS. The MPS peak value occurs in front or behind the tyre footprint when 2m/s^2 acceleration or deceleration is considered, while it occurs at the fore-end of the tyre footprint when considering 4 or 6 m/s^2 deceleration. The locations of the MSS peak values are near to rear-end of the tyre footprint for uniform speed and 2m/s^2 deceleration. When the

deceleration increases to 4m/s^2 or 6m/s^2, the location changes to the forepart of the tyre footprint.

(2) In this study, the MPS at the pavement surface when 6m/s2 deceleration is considered is 1.6 times of that with 4m/s2 deceleration, 2.0 times of that with 2m/s2 deceleration, and 3.5 times of that with a uniform speed. The results for MSS are 1.4 times, 2 times and 34 times.

(3) The vertical distributions of the MPS and the MSS are significantly related to the driving characteristics: the locations of the peak values changes from the sub-surface layer up to the pavement surface with the increases of deceleration rate. The traffic characteristics at the intersection are detrimental to pavement structures particularly in the surface layer.

(4) The complex traffic characteristics at the road intersection will theoretically have significant bearing on the pavement performance or surface distresses, such as fatigue cracking, rutting et al.

Acknowledgements

The authors wish to thank the financial support from the National Natural Science Foundation of China (No. 51178348).

Reference

Alshoaibi, A.M. (2010), "Finite element procedures for the numerical simulation of fatigue crack propagation under mixed mode loading", *Structural Engineering and Mechanics*, **35**(3), 283-299.

Al-Qadi, I.L., Wang, H., Yoo, P.J. and Dessouky, S.H. (2009), "Dynamic analysis and insitu validation of perpetual pavement response to vehicular loading", *Transportation Research Record: Journal of the Transportation Research Board*, **2087**, 29-39.

Cebon, D. (1999), *Handbook of Vehicle-Road Interaction*, Swets&Zeitlinger Publishers.

Dong, Z.J. and Sun, Z.J. *et al.* (2011), "Mechanism analysis of rutting ant urban intersections based on numerical simulation under moving vehicle loads", *Advanced Materials Research*, **152**, 1192-1198.

Elseifi, M.A., Al-Qadi, I.L. and Yoo, P.J. (2006), "Viscoelastic modeling and field validation of flexible pavement", *Joural of Engineering Mechanics*, **132**(2), 172-178.

Hernandez, J.A. (2010), "Evaluation of the response of perpetual pavement at accelerated pavement loading facility: finite element analysis and experimental investigation", Master dissertation, Ohio University, Ohio.

Hu, X.D. and Sun, L.J. (2006), "Mechanistic responses in asphalt pavement under different tyre types with different level loads", *Journal of Tongji University*, **34**(1), 64-68.

Hu, X.D. and Walubita, L.F. (2011), "Effects of layer interfacial bonding conditions on the mechanistic responses in asphalt pavements", *Journal of Transportation Engineering*, **137**(1), 28-36.

Hutchinson, B.G., Rilett, L.R., Green, R. and Haas, R.C.G. (1989), "Axle load shifts during truck braking and their implications for bridge and pavement design", *Canadian Journal of Civil Engineering*, **16**(2), 113-118.

Jo, J.S., Jung, H.J. and Kim, H.J. (2008), "Finite element analysis of vehicle-bridge intersection by an interative method", *Structural Engineering and Mechanics*, **30**(2), 165-176.

Lu, P.Z., Zhao, R.D. and Zhao, J.P. (2010), "Experimental and finite element studies of special-shap arch bridge for self-banlance", *Structural Engineering and Mechanics*, **35**(1), 283-299.

MA, X., Guo, Z.Y. and Yang, Q. (2009), "3D finite element analysis on asphalt pavement dynamic response under moving load", *Journal of Chong Qing Jiaotong University (Natural Science)*, **28**(4), 702-707.

Shan, J.S. *et al*. (2007), "Mechanistic responses in pavement structures considering moving load", *Journal of Highway and Transportation Research and Development*, **24**(1), 10-13.

Siddharthan, R.V., Yao, J. and Sebaaly, P.E. (1998), "Pavement strain from moving dynamic 3D load

distribution", *Journal of Transportation Engineering*, **124**(6), 557-566.
Siddharthan, R.V., Krishnamenon, N., El-Mously, M. and Sebaaly, P.E. (2002), "Investigation of tyre contact stress distribution on pavement response", *Journal of Transportation Engineering*, **128**(2), 136-144.
Siddharthan, R.V., Yao, J. and Sebaaly, P.E. (1998), "Pavement strain from moving 3D load distribution", *Journal of Transportation Engineering*, **124**(6), 557-566.
Tielking, J.T. and Roberts, A.M. (1987), "Tyre contact pressure and its effect on pavement strain", *Journal of Transportation Engineering*, **113**(1), 56-71.
Wang, H. and Al-Qadi, I.L. (2009), "Combined effect of moving wheel loading and three-dimensional contact stress on perpetual pavement responses", *Transportation Research Record: Journal of the Transportation Research Board*, **2095**, 53-61.